

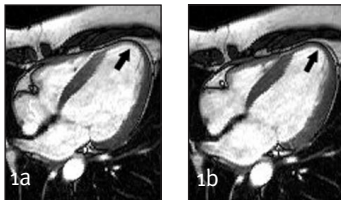
# CLINICAL APPLICATIONS OF CARDIOVASCULAR MAGNETIC RESONANCE IMAGING

Dr Szilard Voros  
Professor Christopher M Kramer

## Cardiovascular magnetic resonance in ischaemic heart disease

### Left and right ventricular size and function at rest

The most fundamental quantitative measurements of the heart include those of ventricular size and function and these measurements are frequently used in clinical decision making. Due to its high spatial and temporal resolution and the freedom to image in any plane, cardiovascular magnetic resonance (CMR) imaging is especially suited for this task. Traditionally, black blood spin echo techniques and bright blood gradient echo cine techniques have been utilised for this purpose, but these have been replaced by the newer steady-state, free precession-based approach, which results in substantially improved blood pool-to-myocardium contrast (see Figures 1A and 1B).<sup>1</sup>



**Figures 1A and 1B.** End-diastolic (A) and end-systolic (B) still frames using steady state, free precession imaging in the four-chamber, long-axis orientation. Note the

excellent blood-pool-to-myocardium contrast and endocardial definition. The end-diastolic image in this orientation is typically used for measurements of LV dimensions. Also, note the apical thinning on the end-diastolic image (arrow in A) and apical hypokinesia on the end-systolic image in this patient (arrow in B).

There are two common approaches to measuring left ventricular (LV) size and function. The faster and less robust approach, the area-length method, relies on two measurements only (LV area and length; LV volume =  $0.85 \times A^2/L$ ), but assumes that the shape of the LV is that of a prolate ellipse, an assumption that does not hold up in remodelled ventricles.<sup>2</sup> The other approach is based on Simpson's rule. Using this method, contiguous short axis slices of the left ventricle are obtained from base to apex, endocardial and epicardial borders are planimeted, volumes for each slice are calculated by multiplying the area by slice thickness and, finally, total ventricular volume is calculated by adding the volumes of individual slices. Myocardial mass is calculated by multiplying myocardial volume by its density.

The advantage of this method is that it is completely free

of geometric assumptions and, therefore, it is more reliable in disease states.<sup>2</sup> Normal values in volunteers have been published for both the left and the right ventricle.<sup>3</sup> As measurements of ventricular size and function are very reproducible with CMR,<sup>4</sup> this allows for smaller sample sizes for clinical studies using these parameters as endpoints. For example, to measure a 3% change in EF in drug therapy of heart failure, 102 patients would be needed by echo and 15 by CMR, a reduction of 85% in sample size.<sup>5</sup>

Myocardial wall thickening is usually calculated by the centreline method, where a line is created in the centre of the myocardium, equidistant from the endocardial and epicardial borders. Multiple chords are placed perpendicular to the centreline between the epicardial and endocardial borders and thickening is calculated as the ratio of the length of the cord at end-systole and end-diastole.<sup>6</sup> To calculate regional myocardial strain, images may be acquired using myocardial tissue tagging, where a grid is placed over the myocardium at end-diastole and regional strain is calculated from the deformation of the grid from end-diastole to end-systole.<sup>7,8</sup>

### Functional stress testing

Regional myocardial dysfunction occurs in patients during pharmacological stress as a result of ischaemia, if a flow-limiting coronary arterial stenosis is present in the artery supplying the myocardial segment. Detection of this regional dysfunction can be used to identify patients with underlying coronary artery disease. Improvements in hardware, the introduction of haemodynamic monitoring and MR-compatible infusion equipment and the development of software platforms allowing for monitoring of myocardial function during stress have made this technique feasible in the MR environment.

Building on these improvements, Nagel et al<sup>9</sup> showed improved sensitivity and specificity for dobutamine MR compared to stress echocardiography and Hundley et al<sup>10</sup> showed that dobutamine MRI stress testing has excellent accuracy in patients who had inadequate acoustic windows for stress echocardiographic studies (sensitivity 83%, specificity 83%). It is important to point out that performing dobutamine MRI stress testing requires a carefully assembled team with adequate nursing support, online monitoring of ventricular function and rhythm during the study, and standardised protocols.

### Myocardial perfusion imaging

Myocardial perfusion is compromised in the presence of a significant epicardial coronary artery stenosis and this

perfusion abnormality can be detected with non-invasive modalities. As a result of coronary arterial autoregulation, resting flow does not become diminished unless the luminal obstruction has reached 90%; however, during maximal vasodilation, perfusion decreases with lesser degrees of coronary stenosis relative to myocardium perfused by normal arteries. Most non-invasive modalities depend on the demonstration of this flow heterogeneity.

For the purposes of CMR perfusion imaging, gadolinium-DTPA (Gd-DTPA) is injected into a peripheral vein at the time of maximal vasodilation and its first pass is imaged through the circulation and the myocardium with relatively high spatial and temporal resolution, covering representative slices of the heart. Gd-DTPA shortens T1-relaxation time and therefore brightens tissues in the compartment where the agents are distributed. The volume of distribution of Gd-DTPA is the extracellular compartment. The typical dose of Gd is 0.025-0.075mmol/kg, injected as a tight bolus by a power injector. Strictly intravascular agents and susceptibility agents (which cause a dark signal on MRI) are also under investigation.

Imaging the first pass of Gd-DTPA can be achieved by fast gradient echo-based techniques, echo planar imaging (EPI), hybrid techniques or by the newer steady state, free precession-based pulse sequences. The EPI readout allows for better anatomical coverage of the left ventricle, but it is more susceptible to ring artifacts at the blood-pool-myocardium interface. The SSFP-based techniques are currently under investigation. Regardless of pulse sequence, images are obtained every heartbeat at several slice positions. Perfusion defects appear as areas of hypointense myocardium, usually in the subendocardium (see Figure 2).



**Figure 2.** First-pass perfusion imaging during the myocardial phase in a mid-ventricular short axis orientation, using an inversion-recovery fast gradient echo pulse sequence. Note the contrast agent in the right and left ventricle and in the ventricular myocardium. There is a well-defined near-transmural perfusion defect in the anterior and anteroseptal regions, which appear as areas of low signal intensity (arrows).

For clinical purposes, images can be analysed qualitatively by visual inspection for the presence of perfusion defects, although the accuracy of visual analysis has not been well validated. Semi-quantitative analysis is usually performed by using a linear fit of the signal intensity curve and comparing it to the input function, generated by a smaller bolus measured in the LV cavity. These semi-quantitative techniques have been validated against PET measures of blood flow, with a sensitivity and specificity of 87% and 85% respectively, compared to quantitative angiography.<sup>11</sup> The accuracy of CMR perfusion imaging is comparable to radionuclide modalities and, in a recent study, had sensitivity

of 88% and specificity 90% versus angiography.<sup>12</sup>

### Imaging of myocardial viability

With the widespread use of percutaneous and surgical revascularisation techniques, determination of myocardial viability has become an important clinical task. Myocardial viability has several definitions, but, from the clinician's perspective, it is defined by the return of contractile function after revascularisation. Traditionally, myocardial viability has been assessed by radionuclide techniques, based on late redistribution of thallium or based on determining counts in the affected myocardial segment compared to areas of maximal counts on Spect imaging. More recently, dobutamine echocardiography has been used for this purpose.

Contrast-enhanced, delayed enhancement imaging for the detection of myocardial viability is a novel and exciting application of CMR. It has been noted since the 1980s that contrast-enhanced MRI can detect areas of myocardial infarction based on high signal intensity, but an improved imaging sequence using inversion recovery has significantly improved the image quality.<sup>13</sup> This technique is based on delayed wash-in and wash-out kinetics of Gd-DTPA into and out of infarcted tissue, compared to normal myocardium.<sup>14</sup> This allows for easy detection of differences in signal intensity between normal and infarcted myocardium, when imaging time after contrast injection is optimised for maximal difference between normal and infarcted tissue (15-20 minutes). Imaging parameters are optimised such that signal from normal myocardium is suppressed and infarcted tissue appears as areas of increased signal (signal intensity ~500% of normal tissue) (see Figure 3).<sup>13</sup> Infarct detection has been validated with this technique in animal models against histology, both in acute reperfused and non-reperfused infarcts as well as in the chronic setting.<sup>15</sup>

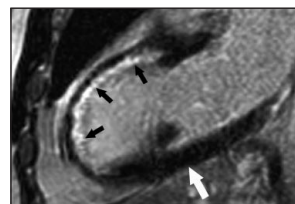


**Figure 3.** Delayed enhancement imaging using an inversion recovery, fast gradient echo-based pulse sequence in the two-chamber, long axis orientation. Signal in normal (non-infarcted) myocardium is suppressed (white arrow). There is an area of extensive, non-transmural hyperenhancement in the subendocardial region of the basal, mid-, and apical anterior wall of the left ventricle, consistent with myocardial infarction (black arrows).

Studies in humans revealed that areas of persistent hypoenhancement (hypointense areas both on first pass images and on delayed enhancement images) represent areas of microvascular obstruction and no-reflow. The presence of this pattern indicates minimal functional recovery after revascularisation and suggests poor prognosis.<sup>16,17</sup> Currently, CMR is the only technique able to resolve the transmural extent of myocardial infarction. This is important, as it has

been shown both in the acute and the chronic setting that the transmural extent of hyperenhancement is inversely proportional to the likelihood of functional recovery after myocardial infarction or revascularisation in chronic ischaemic disease.<sup>18,19</sup> In general, when there is no hyperenhancement, the likelihood of recovery is close to 80%. On the other hand, when the transmural extent of hyperenhancement is more than 75%, the likelihood of recovery is less than 5%. It has also been shown that when the transmural extent of hyperenhancement is between 1% and 50%, functional recovery may not be accurately predicted based on the hyperenhancement pattern alone; contractile reserve in response to low dose dobutamine may be able to distinguish viable from non-viable myocardium in these cases.<sup>20</sup>

### Coronary artery imaging

A most appealing role for CMR in ischaemic heart disease would be the non-invasive assessment of the coronary arteries with high temporal and spatial resolution, during relatively short acquisition times. Coronary magnetic resonance angiography (CMRA) has not matured to that point yet, but substantial improvements have been achieved over the past few years. Given the small size, tortuous course and motion of the coronary arteries, several technical challenges must be overcome in order to obtain images of diagnostic quality. Best in-plane resolution for CMRA is about 700-900 $\mu$ m, which is still about twice the pixel size compared to conventional x-ray angiography.<sup>21</sup> Compensation for cardiac and coronary arterial motion is achieved by using short acquisition times and obtaining images during isovolumic relaxation, which is about 300-400ms after the R-wave at usual resting heart rates.<sup>22</sup> Respiratory motion correction can be achieved by several different techniques. The advantages of conventional breath-holding techniques are shorter acquisition times and the freedom to repeat the acquisition if the images are suboptimal, but the shorter acquisition time results in lower signal-to-noise ratio (SNR). SNR can be greatly improved upon by longer acquisition times, but this requires respiratory compensation to avoid blurring of the images.

The most commonly used techniques rely on diaphragmatic navigators, in which the lung-diaphragm interface is tracked and is used to predict the motion and position of the coronary arteries.<sup>23</sup> Using this method, each acquisition takes about 5-10 minutes with the current navigator efficiency of 30-50% during free breathing.

Many pulse sequences have been evaluated in CMRA. In general, earlier 2-D techniques have been replaced by 3-D acquisition schemes, using mostly bright blood techniques (gradient echo, echo planar and steady state, free precession imaging), in which blood flowing in the coronary arteries generates a bright signal and stenoses appear as signal voids due to local spin dephasing, caused by turbulence in the stenotic segment.

In clinical practice, CMRA is used to assess anomalous coronary arteries, where it has been shown to be equivalent

or superior, compared to conventional x-ray coronary angiography.<sup>24</sup> Other clinical applications include the evaluation of patients with Kawasaki disease<sup>25</sup> and the patency of bypass grafts.<sup>26</sup>

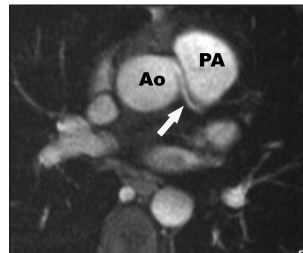


**Figure 4.** Breath-held, 2D, Turbo-FLASH imaging of an anomalous left main coronary artery, arising from the right coronary cusp. Note the course of the left coronary artery (arrow) between the aorta (Ao) and the pulmonary artery (PA).

In the clinical assessment of native coronary artery disease by CMRA, initial reports focused on visualisation of the proximal coronary arteries as well as on SNR and contrast-to-noise ratio (CNR). After many publications of single centre experience with CMRA, a prospective multicentre study was conducted using a single hardware platform with a standardised imaging protocol.<sup>27</sup> Patients were referred for their first diagnostic coronary angiogram and they were imaged during free-breathing using a navigator technique with a 3-D segmented k-space gradient echo sequence. CMRA detected a total of 78 of 94 coronary stenoses found on the conventional angiogram (83%). Sensitivity and specificity for significant stenoses in the LMCA, LAD, LCx and RCA were 67% and 90%, 88% and 52%, 53% and 70%, 93% and 72%, respectively. Sensitivity, specificity and accuracy for the detection of LMCA disease or three vessel disease were 100%, 85% and 87%, respectively. While accuracy was quite high in the diagnosis of LMCA disease or three vessel disease, sensitivity and specificity were suboptimal in individual vessels.

However, with improvements in hardware (e.g. 3-Tesla field strength) and in acquisition techniques (parallel imaging, spiral acquisition, contrast enhancement etc), it is likely that CMRA will become an important non-invasive tool in the diagnosis of coronary artery stenosis.

### Atherosclerotic plaque imaging

Conventional angiographic techniques indirectly detect the presence of atherosclerotic plaques based on their effect on the lumen. Techniques that are able to image plaque directly are important in understanding the pathophysiology of atherosclerosis and ultimately may enable the detection and treatment of vulnerable plaques. MRI's ability to image these plaques noninvasively has made it an attractive tool for this purpose.

MRI of atherosclerotic plaque is based on the principle that different components of the plaque (fibrous cap, lipid core, haemorrhage) create differential signal characteristics on different imaging pulse sequences due to their different relaxation properties. Using a multispectral approach, the same slice is imaged in the same location with different pulse sequences (time-of-flight [TOF], T1-, T2- and PDW-weighted) to identify tissue components. Determination of

plaque volume can be achieved by subtracting luminal area from total vessel wall area and volumes from different slices can be combined.<sup>28</sup> Atherosclerotic plaque characterisation has been performed *ex vivo* and *in vivo* in both animal models<sup>29,30</sup> as well as in humans.<sup>31,32</sup> The use of multispectral CMR to classify atherosclerotic plaques based on American Heart Association class has also been validated.<sup>33</sup> Contrast-enhanced CMR can detect neovasculature in carotid plaques<sup>34</sup> and helps to identify the fibrous cap in aortic<sup>35</sup> and carotid plaque.

CMR can also be used to monitor the effects of lipid-lowering therapies on atherosclerotic plaques. In a case-control study using eight subjects from the FATS trial, it has been shown that prolonged and aggressive lipid-lowering therapy is associated with decreased lipid content and increase in fibrous tissue in carotid arterial plaques.<sup>36</sup> In a prospective CMR study of carotid plaques, simvastatin therapy was associated with increased luminal area, decreased vessel wall area and decreased maximal wall thickness at two years' follow up, indicating reverse remodelling.<sup>37</sup>

## Other common indications for CMR

### Right ventricular cardiomyopathies

Currently, CMR is the best modality for the evaluation of right ventricular cardiomyopathies. A comprehensive exam includes the evaluation of right ventricular and outflow tract size and function and a careful search for intramyocardial fatty tissue. Although the validation of the diagnostic accuracy of these different features is difficult due to the lack of a true reference standard, the presence of focal or diffuse right ventricular or outflow tract dilatation and/or wall motion abnormalities is the most sensitive and specific indicator.

### Pericardial disease

CMR is also one of the best modalities to evaluate the anatomical structure of the pericardium. In general, information about the pericardium and the pericardial space is combined based on signal characteristics on different pulse sequences, including SSFP imaging, T1-weighted imaging with and without fat suppression, T2-weighted imaging and grid tagging. Normal pericardium may not be visualised, but pericardial thickness up to 3mm is normal.<sup>38</sup> Pericardial effusions typically have low signal intensity on T1-weighted, spin-echo images and high signal intensity on T2-weighted and SSFP images. Acute haemorrhagic effusions typically have high signal intensity on T1-weighted imaging as well.

The thickened pericardium of constrictive pericarditis has signal intensity similar to the myocardium, outlined between the bright signal of epicardial and pericardial fat on both T1- and T2-weighted sequences. SSFP-based sequences are not so helpful in the evaluation of the pericardium, but may show increased thickness. In addition to findings consistent with constriction (right atrial and right ventricular enlargement, dilated IVC, sigmoid septum), the presence of

pericardial thickening over 4mm was 88% sensitive, 100% specific and 93% accurate, using cardiac catheterisation and surgical pathology as reference standard.<sup>38</sup> Adherence of the pericardium to the epicardium can be demonstrated by tissue tagging.

### Cardiac and paracardiac masses

A detailed discussion of the detection of cardiac and paracardiac masses is beyond the scope of this review, but a brief introduction to a general approach is outlined below. In general, SSFP-based cine-imaging may be used to evaluate the size and the relationship of the mass to surrounding tissues. A combination of pulse sequences is used for tissue characterisation. Proteinaceous fluid in pericardial cysts has very high signal intensity on T2-weighted imaging. High lipid content (i.e. lipomas) can be easily diagnosed by T1-weighted spin echo sequences, before and after the application of a fat saturation pulse. Vascularity of the mass can be proven by first pass imaging of Gd-DTPA and necrosis is associated with high signal intensity on delayed enhancement images.

Based on a combined approach similar to the one outlined above, CMR has been shown to be very accurate in differentiating benign from malignant tumours.<sup>39</sup>

### Congenital heart disease

A full description of the role of CMR in congenital heart disease (CHD) is also beyond the scope of this review. Evaluation of the patient with CHD requires a very careful and systematic approach. SSFP-based cine-imaging is used to assess chamber size and function as arterio-ventricular connections. For valvular lesions and intracardiac shunts, gradient echo-based cine sequences are often helpful to demonstrate turbulent flow. For further evaluation of shunts, Qp/Qs can be calculated by measuring flow in the ascending aorta and in the pulmonary artery, using velocity-encoded techniques. This technique can also be used to evaluate relative flows in the pulmonary artery branches. Finally, contrast-enhanced 3-D MRA can greatly aid in the evaluation of arterial and venous connections.

## References

1. Barkhausen J, Ruehm SG, Goyen M et al. MR evaluation of ventricular function: true fast imaging with steady-state precession versus fast low angle shot cine MR imaging: feasibility study. *Radiology* 2001; 219: 264-9.
2. Martin ET, Fuisz AR, Pohost GM. Imaging cardiac structure and pump function. *Cardiol Clin* 1998; 16: 135-60.
3. Lorenz CH, Walker ES, Morgan VL et al. Normal human right and left ventricular mass, systolic function and gender differences by cine magnetic resonance imaging. *J Cardiovasc Magn Reson* 1999; 1: 7-21.
4. Bottini PB, Carr AA, Prisant LM et al. Magnetic resonance imaging compared to echocardiography to assess left ventricular mass in the hypertensive patient.

- Am J Hypertens* 1995; 8: 221-8.
5. Bellenger NG, Davies LC, Francis MF et al. Reduction in sample size for studies of remodeling in heart failure by the use of cardiovascular magnetic resonance. *J Cardiovasc Magn Reson* 2000; 2: 271-8.
  6. Van der Geest RJ, Reiber JH. Quantification in cardiac MRI. *J Magn Reson Imaging* 1999; 10: 602-8.
  7. Zerhouni E, Parrish D, Rogers WJ et al. Human heart: tagging with MR imaging. *Radiology* 1988; 169: 59-64.
  8. Axel L, Dougherty L. MR imaging of motion with spatial modulation of magnetization. *Radiology* 1989; 171: 841-5.
  9. Nagel E, Lehmkuhl HB, Bocksch W et al. Non-invasive diagnosis of ischemia-induced wall motion abnormalities with the use of high-dose dobutamine stress MRI: comparison with dobutamine stress echocardiography. *Circulation* 1999; 99: 763-70.
  10. Hundley WG, Hamilton CA, Thomas MS et al. Utility of fast cine magnetic resonance imaging and display for the detection of myocardial ischemia in patients not well-suited for second harmonic stress echocardiography. *Circulation* 1999; 100: 1697-702.
  11. Schwitter J, Nanz D, Kneifel S et al. Assessment of myocardial perfusion in coronary artery disease by magnetic resonance. *Circulation* 2001; 103: 2230-5.
  12. Nagel E, Klein C, Paetsch I et al. Magnetic resonance perfusion measurements for the noninvasive detection of coronary artery disease. *Circulation* 2003; 108: 432-7.
  13. Simonetti OP, Kim RJ, Fieno DS et al. An improved MR imaging technique for the visualization of myocardial infarction. *Radiology* 2001; 218: 215-23.
  14. Kim RJ, Chen EL, Lima JAC et al. Myocardial Gd-DTPA kinetics determine MRI contrast enhancement and reflect the extent and severity of myocardial injury after acute reperfused infarction. *Circulation* 1996; 94: 3318-26.
  15. Kim RJ, Fieno DS, Parrish TB et al. Relationship of MRI delayed contrast enhancement to irreversible injury, infarct age and contractile function. *Circulation* 1999; 100: 1992-2002.
  16. Rogers WJ, Kramer CM, Geskin G et al. Early contrast-enhanced MRI predicts late functional recovery after reperfused myocardial infarction. *Circulation* 1999; 99: 744-50.
  17. Wu KC, Zerhouni EA, Judd RM et al. Prognostic significance of microvascular obstruction by magnetic resonance imaging in patients with acute myocardial infarction. *Circulation* 2003; 97: 765-72.
  18. Choi K, Kim RJ, Gubernikoff G et al. The transmural extent of acute myocardial infarction predicts long term improvement in contractile function. *Circulation* 2001; 104: 1101-7.
  19. Kim RJ, Wu E, Rafael A et al. The use of contrast-enhanced magnetic resonance imaging to identify reversible myocardial dysfunction. *N Engl J Med* 2000; 343: 1445-53.
  20. Bove CM, Jacob MS, Naran KN et al. Dobutamine response by MRI predicts functional recovery after revascularization better than extent of contrast enhancement in chronic subendocardial infarction. *Circulation* 2003; 108.
  21. Yang PC, Meyer CH, Terashima M et al. Spiral magnetic resonance coronary angiography with rapid real-time localization. *J Am Coll Cardiol* 2003; 41: 1134-41.
  22. Sodickson DK, Chuang ML, Khasgiwala VC et al. In-plane motion of the left and right coronary arteries during the cardiac cycle. Proceedings of the International Society for Magnetic Resonance in Medicine 1997; 910.
  23. Taylor AM, Jhooti P, Wiesmann F et al. MR navigator-echo monitoring of temporal changes in diaphragm position: implications for MR coronary angiography. *J Magn Reson Imaging* 1997; 7: 629-36.
  24. Razmi RM, Meduri A, Chun W et al. Coronary magnetic resonance angiography (CMRA): the gold-standard for determining the proximal course of anomalous coronary arteries. *J Am Coll Cardiol* 2001; 37: 380.
  25. Greil GF, Stuber M, Botnar RM et al. Coronary magnetic resonance angiography in adolescents and young adults with Kawasaki disease. *Circulation* 2002; 105: 908-11.
  26. Engelmann MG, Knez A, von Smekal et al. Non-invasive coronary bypass graft imaging after multivessel revascularization. *Int J Cardiol* 2000; 76: 65-74.
  27. Kim WY, Danias PG, Stuber M et al. Coronary magnetic resonance angiography for the detection of coronary stenosis. *N Engl J Med* 2001; 345: 1863-9.
  28. Yuan C, Beach KW, Smith LH et al. Measurement of atherosclerotic carotid plaque size in vivo using high resolution magnetic resonance imaging. *Circulation* 1998; 98: 2666-71.
  29. Worthley SG, Helft G, Fuster V et al. High resolution ex vivo magnetic resonance imaging of in situ coronary and aortic atherosclerotic plaque in a porcine model. *Atherosclerosis* 2000; 150: 321-9.
  30. Fayad ZA, Fallon JT, Shinnar M et al. Noninvasive in vivo high-resolution magnetic resonance imaging of atherosclerotic lesions in genetically engineered mice. *Circulation* 1998; 98: 1541-7.
  31. Shinnar M, Wehrli S, Levin M et al. The diagnostic accuracy of ex vivo MRI for human atherosclerotic plaque characterization. *Arterioscler Thromb Vasc Biol* 1999; 19: 2756-61.
  32. Yuan C, Mitsumori LM, Ferguson MS et al. In vivo accuracy of multispectral magnetic resonance imaging for identifying lipid-rich necrotic cores and intraplaque hemorrhage in advanced human carotid plaques. *Circulation* 2001; 104: 2051-6.
  33. Cai JM, Hatsukami TS, Ferguson MS et al. Classification of human carotid atherosclerotic lesions with in vivo multicontrast magnetic resonance imaging. *Circulation* 2002; 106: 1386-73.
  34. Kerwin WS, Hooker A, Spilker M et al. Quantitative

magnetic resonance imaging analysis of neovascularity volume in carotid atherosclerotic plaque. *Circulation* 2003; 107: 851-6.

35. Kramer CM, Cerilli LA, Berr SS et al. MRI can distinguish plaque components including inflammation in abdominal aortic aneurysm. *Circulation* 2001; 104: 375-6.
36. Zhao XQ, Yuan C, Hatsukami TS et al. Effects of prolonged intensive lipid-lowering therapy on the characteristics of carotid atherosclerotic plaques in vivo by MRI. *Arterioscler Thromb Vasc Biol* 2001; 21: 1623-9.
37. Corti R, Fuster V, Fayad ZA et al. Lipid lowering by simvastatin induces regression of human atherosclerotic lesions. *Circulation* 2002; 106: 2884-7.
38. Masui T, Finck S, Higgins CB. Constrictive pericarditis and restrictive cardiomyopathy: evaluation with MR imaging. *Radiology* 1992; 182: 369-73.
39. Hoffman U, Globits S, Schima W et al. Usefulness of magnetic resonance imaging of cardiac and paracardiac masses. *Am J Cardiol* 2003; 92: 890-5.

Address for correspondence:

Professor Christopher M Kramer  
University of Virginia Health System  
Departments of Radiology and Medicine  
Box 800170  
Charlottesville, VA 22908, USA  
Tel: (434) 243 6060  
Fax: (434) 982 1618  
Email: ckramer@virginia.edu

*Dr Szilard Voros, fellow physician, Division of Cardiovascular Medicine, Department of Medicine, University of Virginia, and Professor Christopher M Kramer, associate professor, Departments of Radiology and Medicine, University of Virginia Health System, Virginia, USA.*

FLEXIBILITY  
OF DOSAGE

1 mg  
4 mg

2 mg

NEW  
FOR  
HYPERTENSION

WELL  
tolerated

COST  
effective\*

**Doxazolin**  
**Doxatan**  
DOXAZOSIN 1, 2, 4 mg Tablets

**DOXAZOSIN**  
- FLEXIBLE  
prescribing for  
**HYPERTENSION** with  
**CO-EXISTING DISEASE**

\* Originator brand

25%

more expensive for  
1mg & 2mg strengths.

Ref MIMS April 2002

Abbreviated Prescribing Information for Doxatan 1 mg, 2 mg & 4 mg Tablets: Composition: Each tablet contains 1 mg, 2 mg or 4 mg doxazosin as doxazosin mesilate. Doxatan 1 mg Tablets: Round, white tablets engraved on one side with D1. Doxatan 2 mg Tablets: Oblong, white tablets engraved on one side with D2 and a scoreline. Doxatan 4 mg Tablets: Oblong, white tablets engraved on one side with D4 and a scoreline. Indications: Treatment of essential hypertension. Posology and method of administration: The usual initial dose is one 1 mg tablet daily. Depending on the response, the dose may be increased after 1-2 weeks to 2 mg once daily, then 4 mg once daily and then 8 mg once daily. The usual maintenance dose is 2 - 4 mg once daily. The maximum dose is 16 mg daily. Use with caution in elderly patients or patients with renal or hepatic insufficiency. The tablets should be taken in the morning with a glass of water. Use in children: Doxatan 1mg, 2 mg or 4 mg Tablets should not be used in children. Contra-indications: Known hypersensitivity to doxazosin or other quinazolines or any other component of the formulation. Lactation. Warnings: Orthostatic hypotension, particularly at the start of therapy. Use with caution in patients with pulmonary oedema due to aortic or mitral stenosis, high output cardiac insufficiency, right ventricular heart failure due to pulmonary embolism or pericardial effusion, left ventricular heart failure with low filling pressure. Use in patients with severe hepatic dysfunction is not recommended. Interactions: Increased anti-hypertensive effect when used with other anti-hypertensive drugs, vasodilation and nitrites. Decreased anti-hypertensive effect when used with non-steroidal anti-inflammatories, estrogens and sympathomimetics. Doxazosin may reduce blood pressure and the vascular effects of disipamine, epinephrine, adrenaline, metaraminol, methoxamine and phenylephrine. Use with caution with other drugs that may influence hepatic metabolism. Doxatan may interfere with the results of some laboratory tests. Effects on the ability to drive: Doxatan may interfere with the ability to drive or use machines, particularly at the start of treatment or when increasing the dose, changing medications or using alcohol at the same time. Pregnancy: Use of doxazosin during pregnancy requires a careful risk-benefit assessment. Undesirable effects: Common: Freshness/nausea, asthma, headache, chest pain, somnolence, dizziness, postural dizziness, giddiness, oedema, palpitations, muscle cramps, constipation, dyspepsia, shortness of breath, nasal congestion, delayed ejaculation, apathy, frequent need to urinate, increased urination and visual disturbances. Less common: facial/general oedema, syncope, facial redness, fever/shivering, weakness, postural hypotension, arrhythmias, peripheral ischaemia, angina pectoris, tachycardia, myocardial infarction, tremor, muscle stiffness, anaemia, increased appetite, alopecia, epistaxis, bronchospasm, cough, pharyngitis, thirst, hypokalaemia, goit, muscle pains, joint swelling/aches, muscle weakness, nightmares, memory loss, emotional lability, incontinence, urinary disturbances, dysuria, abnormal tear flow, photophobia, tremulous, disturbed sense of taste. For other undesirable effects see SPC. Nature and contents of container: Blister pack of 28 tablets. PA 593/20/1-3. PA Holder: Stada AG, Germany. Distributor: Clonmel Healthcare Ltd, Waterford Road, Clonmel, Co. Tipperary. Full prescribing information available on request.

Clonmel Healthcare Ltd, Waterford Road, Clonmel, Co. Tipperary. Tel 052 77777.  
"AVAILABLE ON THE GMS"

where quality costs less